J Therm Anal Calorim (2011) 103:81–88
DOI 10.1007/s10973-010-1170-5

Water evaporation from gel beads

A calorimetric approach to hydrogel matrix release properties

Barbara Bellich · Massimiliano Borgogna · Michela Cok · Attilio Cesàro

AICAT2010 Special Chapter

Abstract Hydrogels are characterized by properties which make them ideal candidates for applications in several fields, such as drug delivery, biomedicine, and functional foods. Molecular diffusion out of a hydrogel matrix depends on their hydrodynamic radii and the mesh sizes within the matrix of the gel. A quantitative experimental and mathematical understanding of interactions, kinetics, and transport phenomena within complex hydrogel systems assists network design by identifying the key parameters and mechanisms that govern the rate and extent of solute release. In this article a calorimetric differential scanning calorimetry (DSC) study reports on the approach to parallel water effusion from a hydrogel matrix to the release of a model protein. The measurement of the water evaporation is taken as the simplest routine determination of a phenomenon that is basically due to a diffusive process through the porous structure of the gel and thermodynamically governed by the difference in the water chemical potential inside and outside of the bead. The analysis of the experimental calorimetric curves is made with the purpose of extracting several numerical parameters characteristic of each curve. The rationale is to develop a simple methodology to understand the release properties of the porous structure of the complex gel matrix by means of DSC.

Keywords DSC · Water effusion · Hydrogel · Beads · Release

B. Bellich (✉) · M. Borgogna · M. Cok · A. Cesàro
Laboratory of Physical and Macromolecular Chemistry, Department of Life Sciences, University of Trieste, via l. Giorgieri, 1-34127 Trieste, Italy
e-mail: bbellich@units.it

Introduction

Hydrogels are characterized by particular properties which make them ideal candidates for applications in several fields, such as drug delivery, biomedicine, and functional foods. The common property underlying the role of hydrogels in many applications is the duality between the polymer network constituting the gel matrix and the diffusible active molecules in the presence of an excess of solvent, most commonly water [1]. In order to achieve a hydrogel system with predetermined and well-defined physico-chemical properties, the knowledge of the polymer network and its solvent interaction is essential [1–3].

There are several complex phenomena that may occur in practice, which allow the diffusible molecules to move from the core into the solvent surrounding the hydrogel network. Although the polymeric network provides a structural framework that holds the liquid in place, also solvent molecules are free to migrate and are redistributed in the external solution, thus resulting in a gel swelling or contraction [4].

To simplify the complexity and to refer to some common experimental conditions, let us limit the analysis of the fundamental literature to hydrogel network with an approximately spherical shape (called bead) with size that ranges from nanometers to millimeters, with a defined chemical potential of diffusible species inside and outside the bead. In the absence of swelling and erosion phenomena, the most common mechanism of molecule release from hydrogels is passive diffusion, where the transport properties of diffusible molecules through the polymer network are regulated by the chemical potential and by the permeability of the network. In the case of three components only, polymer network, solvent water, and a diffusible molecule, the self-diffusion coefficient for a given

diffusing molecule depends both on its own size and the size of the obstacle present in the bead, due to the motionless polymer network [5]. This concept is well known, inasmuch diffusion of small molecules is not considerably retarded in a swollen state gel, whereas macromolecules with high hydrodynamic radius, like large globular proteins, will have a delayed release [2]. Less clear is the effect of the presence of several complex interactions between the diffusible species and between them and the matrix. Thus, a quantitative understanding of structural material properties, interactions, and kinetic events within complex hydrogel systems allows identifying the key parameters and the overall mechanisms that govern the rate and extent of the release of diffusing molecules [5].

Many studies in the literature report on theories and on physical model of diffusion, based on the effects of obstruction, free volume, and hydrodynamic interactions, in systems with the presence of additional components such as polymer fillers. On the assumption that the self-diffusion coefficients of polymer components is always much smaller than that of the diffusing ones, the polymer chains of the fillers can be considered motionless with respect to the diffusion of solvent and solutes. As a consequence, the polymers create an overall fixed and impenetrable network immersed in a solution thus leading to an additional increase in the path length for the molecules in motion [5]. Most models identify the polymer volume fraction as the key parameter that governs the diffusion process of diffusing molecules of defined geometry.

In order to limit the complexity of the description of small molecules diffusion from a hydrogel bead made of a network of interpenetrated polymer chains, simplified conditions are required. In addition, a treatment that can be applied to all molecules as a function only of their size and independent on the other properties would be desirable. This study reports the progress of a calorimetric study on dehydration process of alginate beads [6], focusing on the diffusion of water molecules out from the matrix structure, in order to understand the validity of the calorimetric approach as a predicting tool for the diffusion of solutes.

Materials and methods

Materials

The preparation of alginate gel beads was carried out employing the following materials: Alginate from brown algae ($F_G = 0.4$, $[\eta] = 4.3$ dl/g in aqueous 0.1 M NaCl) obtained from Sigma-Aldrich Co. (St. Louis, Mo). Two types of hydroxypropylmethylcellulose (HPMC) with the same substitution degree but different molecular weights were used: HPMC MP843 Benecel ($[\eta] = 7.1$ dl/g in water; Hercules Doel B.V.B.A Aqualon Division) and HPMC K100 M Methocel ($[\eta] = 11.6$ dl/g in water; Dow Chemical Company). Some samples contained also chitosan with low molecular weight ($[\eta] = 4.9$ dl/g in aqueous acetate buffer 0.25 M pH 4.7) obtained from Sigma-Aldrich Co. (St. Louis, Mo). Lysozyme (E.C. 3.2.1.17, Sigma Chemical Co) was used as a model protein. Other reagents used were: sodium acetate (Sigma Chemical Co), acetic acid (Sigma Chemical Co), and calcium chloride dehydrated (Aldrich Chemical Co. Milwaukee, WI).

Preparation of beads

A model system for the assessment of the influence of the various components contained in a formulation has been developed. The model system consists of alginate gel beads. The beads are obtained by simple dropping of an alginate solution (2% w/v) with a syringe in a gelling solution consisting of calcium chloride 50 mM. The beads were collected after 10 min under mild mixing. Some samples were prepared by adding different biopolymers, such as HPMC, to the starting alginate solution. Beads with chitosan were also prepared by dropping alginate in the gelling solution containing chitosan dissolved in an acetate buffer.

Differential scanning calorimetry (DSC)

A heat flux calorimeter (mod. DSC6, Perkin Elmer Instruments) was used for analysis. One sphere was placed in an open pan and analyzed, under nitrogen flux (20 ml/min), in the temperature range from 287 to 403 K (or 433 K, depending on the sample) at the scanning rate of 5 and 10 K min^{-1}. The spheres were weighed before and after DSC analysis in order to calculate the amount of water and the dry matter. Data collection was carried out with the software Pyris (Perkin Elmer) and data analysis was performed with the software Origin® 6.0. All measurements were repeated at least in triplicate on bead samples from the same freshly prepared batch.

Results

Model alginate beads

Among the several samples based on alginate gel beads studied in our laboratory, those here investigated are reported in Table 1, together with other relevant properties. From a morphological point of view, the beads made with only calcium-alginate are generally characterized by a spherical and regular shape and their appearance is transparent. The diameter of the beads prepared according to the

Table 1 Main characteristics of gel beads: sample, value of the slope (*B*), ratio calculated (*F*) of B values, enthalpy of evaporation $\Delta H/Jg^{-1}$, fraction of area 1 (Xa1), heat flow at 35 °C relative to alginate solution ($100 \times HF/HFa$), fraction of polymer in bead (Φp), and release percentage of lysozyme from beads after 1 h

	Sample	*B*/*K*	*F* = B/Ba	$\Delta H/Jg^{-1}$	$100 \times X_{a1}$	$HF/HFa \times 100$	Φp	Release %
a	Alginate solution	−4489	1	2764	100	100	0.010	–
b	Alginate	−3662	0.82	2508	97	74	0.034	48.1
c	Alginate + HPMC MP843 0.25% w/v	−3743	0.83	2288	94	67	0.031	48.9
d	Alginate + HPMC MP843 1% w/v	−3207	0.71	2304	88	37	0.031	35.9
e	Alginate + HPMC K100 M 0.25% w/v	−3597	0.80	2359	94	52	0.036	59.6
f	Alginate + HPMC K100 M 1% w/v	−3454	0.77	2261	92	37	0.030	37.5
g	Alginate + Chitosan	−3236	0.72	2177	88	30	0.037	15.5
h	Alginate + HPMC MP843 0.2% + Chit	−3101	0.69	2278	90	30	0.028	26.0

See text and equations for details. Data of alginate solution are also reported

experimental conditions is around 2–3 mm. The addition of other components produces some loss of transparency, especially in the case of lysozyme. This optical effect clearly points out the heterogeneous texture of the gel matrix of blended semicompatible biopolymers. Moreover, often the beads produced with HPMC are no more regular spherical in shape and are characterized by a small tail which is due to the change in rheological properties of the dropping solution (see Fig. 1 of ref [7]).

Differential scanning calorimetry: preliminary observations

The alginate gel beads were analyzed by differential scanning calorimetry at two scan rates 5 and 10 K min^{-1} as reported in Fig. 1. Measurements have been carried out by exploring the evaporation process of the water contained in the beads from room temperature to the end of thermal events associated to water, approximately 400 and 440 K for scan rate 5 and 10 K min^{-1}, respectively. For comparison purpose, the thermogram of an alginate solution at the same polymer concentration is also reported. Being water the major component (up to 97.5% w/w), most of the thermal event can be associated to the evaporation process of "free" water, although more or less constrained during the diffusion by the dimension of the gel bead pores. As a consequence, all the thermograms are characterized in the first part by the typical exponential growth of the heat flux as a function of the temperature. A slower increase of the heat flux is observed for the more complex beads, while for the alginate solution the increase in heat flux is quite rapid. Therefore, the first part of the evaporation curve was considered characteristic of the type of the bead sample. The evolution of the slope depends of the composition of the matrix; the addition of various components clearly

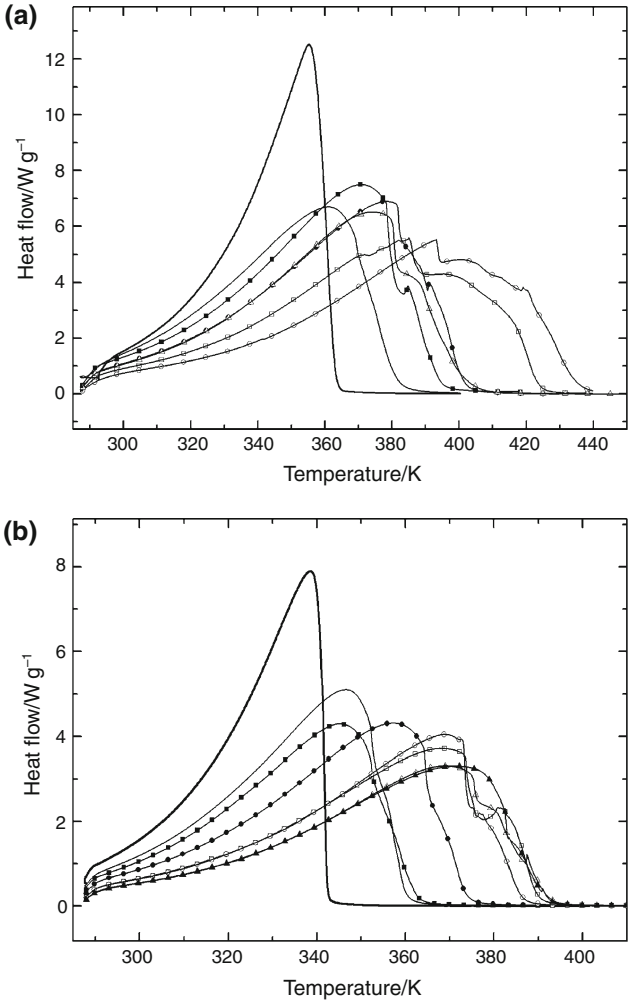

Fig. 1 Thermograms of vaporization enthalpy of water from beads. Letters refer to samples listed in Table 1: *b* (*full line*), *c* (*filled square*), *d* (*open square*), *e* (*filled circle*), *f* (*open circle*), *g* (*open triangle*), and *h* (*filled triangle*) at scan rate 10 K min^{-1} (*top*) and scan rate 5 K min^{-1} (*bottom*). Alginate solution (*a*) is reported for comparison (*bold line*)

affects the slope and, as a general rule, the simplest the system the highest the slope. A distinct well-defined peak was recorded only in the case of the alginate solution, because of the abrupt fall down of the heat flux after the maximum, due to the exhaustion of water evaporation process. All the other samples, in particular those corresponding to alginate beads containing HPMC or chitosan, are characterized by a broad peak. Furthermore, for these complex systems water evaporation is not yet completed right after the peak, and a broader decline of the curve is observed and attributed to the delayed evaporation of the remaining bound water. Thus, quite a few relevant differences are found also in the last part of the curves when the evaporation process is going to be completed. It is evident that the heat evolution in the final part of the DSC curve may not strictly follow the mass weight change as that measured by thermogravimetry. For the purpose of this study and for the differences that occur in DSC and thermogravimetry, a separate study will have to be carried out by TGA.

The qualitative observations made so far are valid for both the scan rates investigated. Indeed, some different behaviors in the ranking were found between the two scan rates and it was observed that scanning at 10 K min^{-1} produces a spreading of the curves that is not found at scan rate 5 K min^{-1}. However, the results at low scan rate put more emphasis on the quasi-equilibrium evaporation process, while the high scan rate favors the non-equilibrium part. In addition, the lowest scan rate provides more reproducible thermograms especially in the second part of the evaporation curves where at scan rate 10°/min some peculiar behaviors are occasionally noticed such as the jumping of the beads out of the DSC pan. This phenomenon, named as "pop corn" effect, has already been reported for the dehydration process of gel beads measured by thermogravimetry [8]. In conclusion, in this study the full quantitative analysis of the thermograms is restricted to those recorded at scan rate 5 K min^{-1}.

Model development

Basic theory

The evaporation rate of a liquid at a droplet surface depends on geometrical and thermodynamic parameters. The rate of mass transfer (kg.s^{-1}) is:

$$dm/dt = \gamma A M/R\left(P_d/T_d - P_\infty/T_\infty\right) \approx \gamma A M \Delta P/RT \quad (1)$$

where γ is the mass transfer coefficient, $A = \pi d$ is the surface area of the droplet, R is the universal gas constant, M is the liquid molecular weight, T_d (P_d) is the temperature (partial pressure) of the vapor in equilibrium within the droplet, T_∞ (P_∞) is the external vapor temperature (partial pressure) [9]. The simplification $T_d \approx T_\infty = T$ can be easily made for thermal equilibrium conditions. The presence of co-solutes needs to be taken into account in the change of the solvent chemical potential, which is the effective driving force for the evaporation process. If the Flory–Huggins model is accurate enough to describe the chemical potential of a solvent in a mixture in the presence of polymeric cosolutes,

$$\mu_1 = \mu_1^\circ + RT\left(\ln(1-\varphi_2) - \chi\varphi_2^2 + \varphi_2\right) \quad (2)$$

then the polymer/solvent binary mutual-diffusion coefficient D can be derived [10].

The claim is that DSC is a suitable methodology to measure in a simple way the temperature dependence of the mass transfer of a liquid phase (i.e., water) from the bead to the vapor phase. Thus, the experiments give both kinetic and thermodynamic data about the transfer process.

Starting from the concepts illustrated in the Introduction and in the references therein quoted, a simple molecular thermodynamic model has been devised to analyze the evaporation behavior presented in the previous section.

The model alginate bead is characterized by a spherical symmetry with an effective curvature that can be considered planar for the purpose of this treatment (no edge or roughness effects). Under these circumstances, several chemical potential profiles could in principle be attributed to the component water on the basis of the chemical and structural characteristics of the gel matrix and of the additional polymers added in the bead formulation. A schematic plot of the concentration profile (and, therefore, of the chemical potential) of water is given in Fig. 2 for four different thermodynamic models:

(a) uniform water droplet
(b) uniform gel particle
(c) layered capsule
(d) realistic gel bead

The instantaneous rate of evaporation at the droplet surface depends on the composition and structure of the droplet. Both c and d are realistic chemical potential variations in real cases. Indeed, the profile of the chemical potential and, therefore, the instantaneous evaporation rate at constant temperature is a function of the time for all the gel models.

To complete this short analysis of the dependence of mass transfer rate on the operational parameters of the process, reference is made to the effect of the dimension of pores through which water may flow out of a confined compartment. This concept simply comes out from inspection of Eq. 1 through an extension of the meaning of the parameter A. Indeed, experimental results collected on

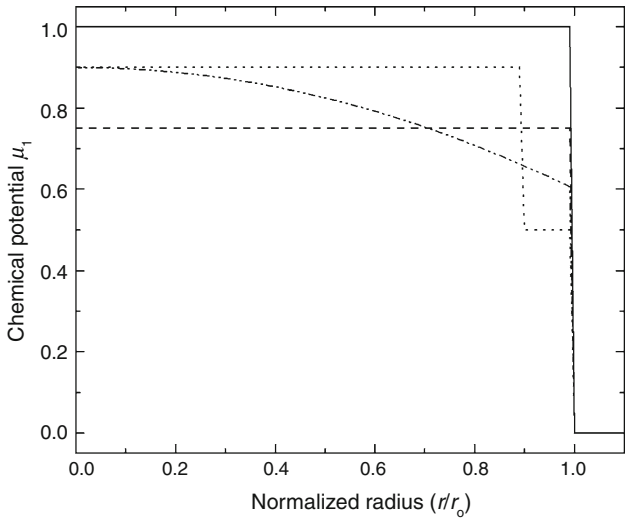

Fig. 2 Schematic dependence of the solvent chemical potential according to bead models a–d. Water drop (*solid line*), capsule (*dotted line*), real bead (*dashed dotted line*), and uniform gel(*dashed line*)

water droplets at scan rate of 10 K min^{-1} show a linear dependence of the *HF* at 35 °C as a function of the dimension of the hole of the calorimetric pan, from 0.1 to 1.2 mm of diameter [11]. In isothermal conditions this dependence is equivalent to say that the evaporation rate is effectively proportional to the "free" surface from which water effusion occurs. Thus, the different models depicted in Fig. 2 can be efficiently rationalized in terms of a single operative parameter, which is a measure of the average pore size through which the water escapes from the bulk in given conditions of temperature and chemical potential gradient. In this way, the kinetic and thermodynamic contributions to the evaporation process are made explicit and the formal separation allows the calculation of structural parameters that influence the phenomenon.

In the following section, a simple preliminary analysis of the experimental calorimetric curves of Fig. 1 is made with the purpose of extracting several numerical parameters characteristic of each curve.

Differential scanning calorimetry: mathematical fitting

Before approaching a mathematical analysis, let us put forward the final scope of the method as briefly outlined at the end of the Introduction. The measurement of the water evaporation is taken as the simplest routine determination of a phenomenon that is basically due to a diffusive process through the porous structure of the gel and thermodynamically governed by the difference in the water chemical potential inside and outside of the bead. This sort of measurement can be done either isothermally or non-isothermally. The non-isothermal measurement provides a non-equilibrium exponential growth that follows the equation:

$$p = a' p^{\circ} e^{T/b} \tag{3}$$

where in equilibrium condition for pure water $a' = 1$ and $b = \Delta H/R$ with $\Delta H = 44.01$ kJ/mol at 25 °C.

It is here claimed that under the present experimental conditions the parameters a' and b contain the quantitative descriptors of effective gel mesh that obstructs the free evaporation of water. The term a' is also function of the scan rate. Although a logarithmic expression is more familiar in the conventional linear form of the Clausius equation (or its approximated Clausius–Clapeyron), from the practical point of view the exponential Eq. 3 is more suitable for a computer-fitting analysis of the experimental data points of the heat flow (*HF*) as a function of the temperature T.

For our systems the parallel equation is used, with the fitting parameters a, b, and HF_o:

$$HF = HF_o + a e^{T/b} \tag{4}$$

The two reasons for this choice are the existence of a residual baseline shift (HF_o) and the experimental noise-to-signal that would overweight data points at lower temperature. In practice, the initial part of the thermogram is fitted in a defined range of temperature (292–330 K) for a total of 60 data points, to limit the fit to the region with almost negligible change in the sphere diameter. The fitted exponential curve is also used as extrapolation to lower temperatures, where experimental data were not collected. The choice was made to avoid freezing of the beads, although this systematically cuts the experimental curve in the lower temperature range.

Analysis of the parameters

Once the experimental curve is fitted and the initial part reconstructed, it is also possible to evaluate the full area underlying the heat flow curve. It was also found that in the majority of the curves a linear extrapolation to $HF = 0$ at temperature of 240 K provides a reasonable approximation for the evaluation of the total heat of evaporation. An example of a typical fitting with the low temperature extrapolation (including the linear one) and the fitting equation is reported in Fig. 3.

For a graphical comparison of the experimental data, the linear form of the equation was used, the exponential equation turned into a logarithmic form as follows: $\ln(HF–HF^{\circ}) = \ln A + B/T$. By plotting the left term versus $1/T$ (Fig. 4), it is possible to calculate the slope of the curve. According to the equilibrium conditions of the Clausius–Clapeyron equation, the slope of such an equation should have the meaning of a reduced evaporation

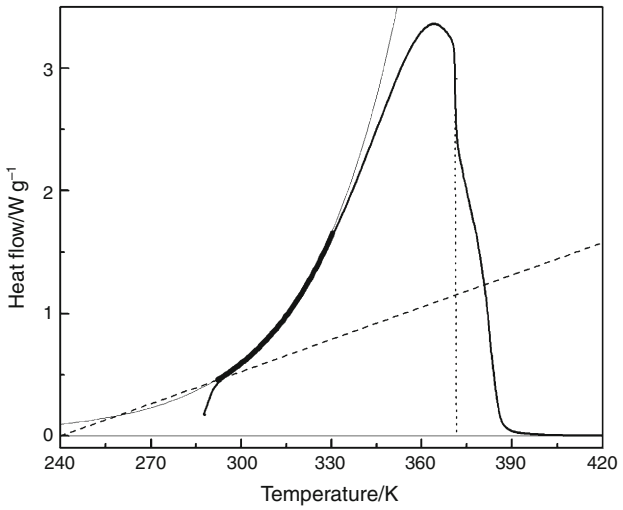

Fig. 3 Example of fitting of a calorimetric curve: exponential curve (*full line*), exponential fitting (*bold line*), extrapolation curve (*dashed line*), and area partition (*dotted line*)

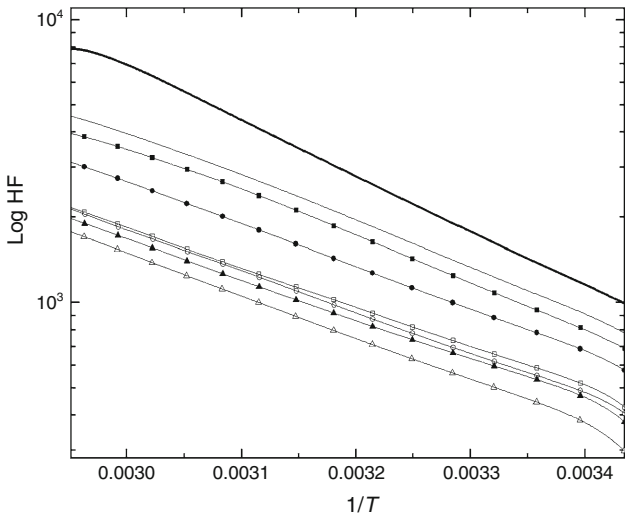

Fig. 4 Linearization of the exponential curves recorded at scan rate 5 K min^{-1}

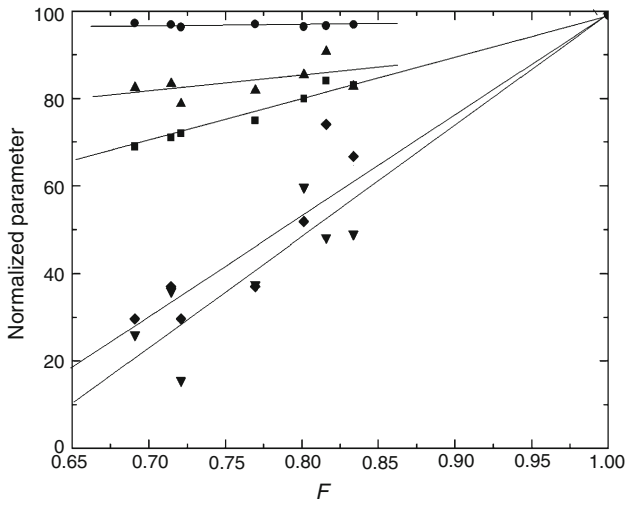

Fig. 5 Plot of fraction of area 1 X_{A1} (*filled square*), vaporization enthalpy of water ΔH (*filled triangle*), fraction of water (*filled circle*), release of lysozyme from beads after 1 h (*filled inverted triangle*), and heat flow at 35 °C (*filled diamond*) as a function of the parameter F = B/Ba. *Lines* are drawn as eye guidelines

enthalpy $\Delta H/R$, while it must be clear that here the slope is modulated by the non-equilibrium conditions (evaporation rate and scanning rate). Effectively, the ratio of these two streaming variables can be chosen to amplify the differences in the evaporation rates from gel beads with different structure.

Another heuristic result is the fact that the value of B (slope) can be averaged over the linear fitting of the set of curves belonging to the same system (column 3 of Table 1).

The slope B decreases with the increasing complexity of the alginate matrix. As expected, water evaporation from a non-gelling system is faster than for any other gel beads, and therefore, the highest value of slope is observed for the alginate solution. The lowest value of the slope is found for the alginate/chitosan/HPMC beads, thus suggesting a slower evaporation rate. The values of all the other systems lay in between. The slope of each sample has been normalized by the value of the alginate solution (Table 1 column 4); the ratio (named parameter F) is an effective measure of the degree of complexity of the alginate matrix. The meaning of the parameter F is not necessarily structurally defined, but the parameter can be operatively used to classify the system under investigation in terms of the higher difficulty of water molecules to diffuse from the liquid to the vapor phase.

Figure 5 reports some features of the systems described also in Table 1, which have been collected and analyzed as a function of the parameter F. Each set of data has been normalized for the highest value, which arises from the reference alginate solution.

The area under the curve is a measure of the total heat involved in the process of water evaporation (column 5). As reported in Table 1, the vaporization enthalpy of water from the alginate solution is the highest, followed by that of the alginate bead, while the values of vaporization enthalpy of all the other beads were constantly lower by 15–20%. The change in the vaporization enthalpy is related to the composition of the system and reflects some small variations in the vaporization process from the thermodynamic point of view. Indeed, the distribution of the overall process of water evaporation is shifted to higher temperature. This shift of the maximum value of the experimental curves to higher temperature implies that there is a small

variation of the heat capacity difference of the vapor and liquid phase, depending on the composition of the system.

The thermogram of the samples displays an initial curve with a common exponential form and is characterized by a final tail which is not present in the alginate solution. The extension of the tail seems to be highly influenced by the composition of the matrix. An approximation has been adopted for the very initial part of the curve, as already mentioned in the section of the mathematical fitting. The area under the curve has been divided into two fractions selecting a border line approximately right after the highest point of the curve, where the evaporation of the fraction of free water is completed (fraction Xa1 reported in column 6 of Table 1). An example of the integration of the two fractions of area is reported in Fig. 4.

Regarding the alginate solution, the area of the second fraction (Xa2) is nearly zero as long as all the water freely evaporates and it is not restrained by the matrix. Regarding the beads, a decrease of fraction Xa1 was found with increasing F, while in parallel fraction Xa2 increases. This is a signature that by increasing the complexity of the matrix structure an increase of the fraction of bound water is observed and the evaporation of water is delayed to higher temperatures. Similarly, given the dependence of the heat flow on the hole size [11], the value of the instantaneous heat flow at a given temperature (e.g., at 35 °C) can be taken as an effective measure of the "conventional pore size" through which water evaporates from the system. The value of HF at 35 °C normalized for that measured for the alginate solution is reported in column 7 of Table 1. Last column of Table 1 reports the polymer fraction in the beads, measured as dry weight fraction after the dehydration in the calorimeter. This fraction in more concentrated gel systems is an effective index of crowding; in very dilute polymer gels it does not really affect the process of water effusion which depends from the quality and the functional structure of the polymer more significatively than the polymer concentration itself.

Comparison with release data

In a parallel study, a study was carried out on the stability and the release of a model protein (lysozyme) from the alginate beads of this study [12]. Release data collected in Tris buffer medium were analyzed as a function of time up to 6 h. In order to compare the samples, the raw release data at the time of 1 h have been included in Fig. 5 and reported in Table 1 (column 9). Within the experimental errors, the release data are characterized by delay which is a function of the increasing complexity of the matrix, measured by the parameter F. This means that the release property correlates also with any of the other parameters listed in Table 1.

Although encouraging, more data are required on several bead samples characterized by different parameter F and also observations should be made with proteins characterized by different physico-chemical properties, such as the degree of hydrophilicity and the isoelectric point. As a consequence of widening the system complexity, the validity of using the DSC analysis, instead of the TGA, will also have to be confirmed.

Discussion and conclusions

The rationale for this study is to understand the release properties of the porous structure of the alginate gel matrix by means of DSC. In a previous study [6] the status of water within the alginate gel bead, proposed as a model system, was described by analyzing the freezing and melting behavior of water. Furthermore, the phenomenological aspects of water evaporation from alginate beads were described for similar systems [7]. In this study, a quantitative approach is set down. The shape of thermograms of spherical samples dramatically differs from the thermogram of a reference alginate solution. While the total heat involved in the evaporation process does not significantly differ within the samples, the rate of the process (shown by the initial part of the curve) clearly reflects the more or less complex composition of the hydrogel matrix and the scan rate becomes an operative parameter. Indeed the average slope of the curve at scan rate 10 is about 80% of those for scan rate 5. This means that we are dealing with a scan rate range that effectively modulates the two non-equilibrium processes: the first is an effect of the scan rate and the second depends on the obstruction. The unbalance between these two variables produces differences that would not be detected at the equilibrium [13]. This observation reinforces the choice of the non-isothermal measurements by DSC. The parameter F, being normalized for a fixed system, should be scan rate-independent in a proper interval of scan rates.

From the experimental point of view, the measured heat flow reflects the difference in vapor pressure existing at the surface of the sphere. The dependence of the heat flow from the dimension of the orifice through which water effusion occurs was already described elsewhere [11]. A linear dependence of the heat flow measured at 35 °C with the square of the orifice radius was found. This concept can be extrapolated to the present gel beads if the volume of the bead remains constant during the whole evaporation process and destructuring effects on the matrix are negligible. Given this premise, water effusion from the alginate is expected to be dependent on the pore size of the gel. As far as the gel considered is a real non-homogeneous system, but rather characterized by an intricate matrix resulting

from polymers entanglement, the rate of water effusion is mainly affected by the obstructions within the matrix, which in the present case does not simply depends on the polymer concentration. In turn, the rate of water evaporation can be considered a measure of the index of solute diffusion.

Several parameters show congruent relationships and indicate that the dependence of molecular mobility can be ascribed to the structural complexity of the gel beads as measured for example by the instantaneous heat flow, or by the slope of the linearized heat flow evolution. In this study the choice has been made to increase the structural crowding by the addition of hydrophilic polymers (chitosan and HPMC) and not by changing the degree of reticulation of the alginate matrix, in order to avoid excessive changes in the ionic properties. Chitosan is commonly employed in combination with alginate in order to reinforce the gel matrix by forming polyelectrolyte complexes [14]. HPMC is commonly used as a polymer generating swellable matrix, since undergoes a glassy-rubbery transition as water penetrates and a gel layer is induced until a saturation state is reached. In the swellable matrix following further interactions with water, the dissociation of the entangled polymer chains leads to dissolution and disintegration of the structure [15, 16]. The systems of this study are already in a gel state; therefore, it is reasonable that the main effect of the HPMC concerns an obstruction contribution like a high molecular weight polymer filler.

In conclusion, the main advantage of the approach outlined here is that the proposed calorimetric analysis is fast enough to insure accurate and reproducible determinations of parameters that are correlated with the release of solvent and of proteins, although it remains to prove that is valid also for small molecules of intermediate dimensions [17]. The need of a certain number of repetitions required in order to have a mean behavior representative of the evaporation curve is not different from that necessary for other type of release measurements. Some drawbacks are apparently present, inasmuch water migrates out of the matrix and a contraction of the polymer structure occurs. Nevertheless, this turns to be a relevant phenomenon that also differentiates the different gel matrices used and provides additional information on the bead deswelling process. The detail analysis of the contribution of the polymer fraction as a function of the total volume of the bead during the evaporation of water needs a larger number of systems, characterized also from other structural point of view. Work is in progress along these lines.

Acknowledgements The present results have been achieved in part within the EU Project FP6 NanoBioPharmaceutics (NMP 026723-2), and the Project ''Oral vaccine carrier for fish farming of Friuli Venezia Giulia".

References

1. te Nijenhuis K. Thermoreversible networks. Viscoelastic properties and structure of gels. In: Advances in polymer science, vol 130; 1997.
2. Hamidi M, Azadi A, Rafiei P. Hydrogel nanoparticles in drug delivery. Adv Drug Deliv Rev. 2008;60:1638–49.
3. Hatakeyama H, Hatakeyama T. Interaction between water and hydrophilic polymers. Thermochim Acta. 1998;308:3–22.
4. Chan AW, Neufeld RJ. Modeling the controllable pH-responsive swelling and pore size of networked alginate based biomaterials. Biomaterials. 2009;30:6119–29.
5. Masaro L, Zhu XX. Physical models of diffusion for polymer solutions, gels and solids. Prog Polym Sci. 1999;24:731–75.
6. Bellich B, Borgogna M, Carnio D, Cesàro A. Thermal behavior of water in micro-particles based on alginate. J Thermal Anal Calorim. 2009;97:871–8.
7. Borgogna M, Bellich B, Zorzin L, Lapasin R, Cesàro A. Food microencapsulation of bioactive compounds: rheological and thermal characterisation of non-conventional gelling system. Food Chem. 2010;122:416–23.
8. Chambree D, Iditioiu C, Segal E, Cesàro A. Non-isothermal behavior of acrylic ion-exchange resins. J Thermal Anal Calorim. 2005;82:803–11.
9. Straatsma J, van Houwelingen G, Steenbergen AE, de Jong P. Spray drying of food products: 1. Simulation model. J Food Eng. 1999;42:67–72.
10. Jiang WH, Han R. Prediction of solvent-diffusion coefficient in polymer by a modified free-volume theory. J Appl Polym Sci. 2000;77:428–36.
11. Sussich F, Bortoluzzi S, Cesàro A. Trehalose dehydration under confined conditions. Thermochim Acta. 2002;391:137–50.
12. Cok M, Bellich B, Borgogna M, Cesàro A. How to improve stability and release of alginate hydrogel beads as biodrug delivery systems. XII CSCC Pontignano (Italy), June 20–23, 2010.
13. Janković B, Adnađević B, Jovanović J. Isothermal kinetics of dehydration of equilibrium swollen poly(acrylic acid) hydrogel. J Thermal Anal Calorim. 2008;92:821–7.
14. Gåserød O, Sannes A, Skjåk-Bræk G. Microcapsules of alginate–chitosan. II. A study of capsule stability and permeability. Biomaterials. 1999;20:773–83.
15. Lee DW, Hwang SJ, Park JB, Park HJ. Preparation and release characteristics of polymer-coated and blended alginate microspheres. J Microencapsulation. 2003;20:179–92.
16. Joshi SC, Chen B. Swelling, dissolution and disintegration of HPMC in aqueous media. In: CT Lim, JCH Goh, editors. ICBME 2008 Proceedings 23; 2009. pp. 1244–1247.
17. Pluen A, Netti PA, Jain RK, Berk DA. Diffusion of macromolecules in agarose gels: comparison of linear and globular configurations. Biophys J. 1999;77:542–52.